Multi-intensity Bending Eavesdropping Detection and Identification Scheme Based on the State of Polarization

Qing Lei, Yajie Li, Haokun Song, Wei Wang, Yongli Zhao, Jie Zhang
Beijing University of Posts and Telecommunications
Beijing 100876, China
jie.zhang@bupt.edu.cn

Yongyuan Liu
Beitsing Communications Technology Co., Ltd.
Beijing 100088, China

***Abstract*—Bending eavesdropping induces fast polarization state transients. We propose a detection scheme for bending eavesdropping, enabling physical layer protection. The accuracy of identifying multi-intensity bending eavesdropping reaches 95.38% by calculating the polarization rotation angular rate.**

Keywords—polarization, Stokes parameters, eavesdropping detection, optical fibers, fiber bending.

I. INTRODUCTION

As an essential part of modern communication, the security of optical communication is crucial, especially the physical layer security. Common attack methods for the physical layer include fiber bending, in-band and out-of-band crosstalk, Repeat-Back Jamming, *etc.* [1]. Among them, fiber bending is a covert eavesdropping attack, in which eavesdroppers intercept transmitted data by applying bending, squeezing and other deformations to the fiber to cause signal leakage.

The majority of attack methods result in power anomalies in the signal. Detection methods often target these power anomalies, such as monitoring the loss distribution along the fiber using the optical-path backpropagation algorithm [2], or identifying signal power distribution anomalies by observing the change of fiber nonlinear noise intensity during propagation [3]. In addition, several detection schemes are designed for specific attack methods. A machine learning framework for in-band out-of-band jamming signal insertion attack detection and identification of physical layer attacks [4]. Machine learning is also used to detect splitting eavesdropping [5]. Compared with other attacks, fiber bending causes a slight loss of power, so power's fluctuation is not the best indicator for detecting bending eavesdropping. In the existing bend eavesdropping detection methods, only bend eavesdropping with bend diameter less than 20 mm [6] or attenuation above 1.5 dB [7] can be identified, which cannot be applied to all bend eavesdropping cases. Polarization is proved to be very sensitive to fiber geometry [8] and therefore is appropriate for bending eavesdropping detection. While performing fiber bending eavesdropping, the geometry of the fiber is bound to change, so bending eavesdropping can be detected based on the state of polarization (SOP) change of the signal [9]. The judgment criterion for eavesdropping is that the first-order difference of the Stokes parameter exceeds the sensitivity threshold. However, intensity of each bending operation is different, leading to different variations of SOP parameters. To achieve higher precision in detecting multi-intensity bending eavesdropping, more comprehensive parameters need to be explored, and more generalized threshold judgment schemes need to be designed.

In this paper, fiber bending eavesdropping with different bend radius is implemented in the basic 20 km end-to-end fiber communication system. We present a detection scheme for multi-intensity bending eavesdropping, including a complete process of thresholds selection. The angular rate of the polarization rotation is calculated using the SOP parameters, which is adopted as the detection parameter. The proposed method achieves 95.38% detection accuracy with experimental data.

II. BENDING EAVESDROPPING DETECTION PRINCIPLE

A. Polarization properties of light and Stokes parameter

Light as an electromagnetic wave, any electric field vector perpendicular to the direction of propagation Z can be decomposed into two orthogonal vectors in the X and Y directions, thus the electric field vector can be represented by the vector sum of the two orthogonal components E_x and E_y :

$$\begin{bmatrix} E_x(t) \\ E_y(t) \end{bmatrix} = \begin{bmatrix} A_x e^{j(\omega t+\varphi_x)} \\ A_y e^{j(\omega t+\varphi_y)} \end{bmatrix} \tag{1}$$

where A_x and A_y are the amplitudes of the orthogonal fields, ω is the angular frequency of the light, φ_x and φ_y are the initial phases of the orthogonal fields.

For light waves, the SOP describes the direction of the electric field vibrations in the light wave. The SOP can be described using different representations, and several commonly used representations are Stokes parameters, Jones vector and Mueller matrix. The method used to describe the SOP in this paper is the Stokes parameters. The Stokes parameters includes four parameters (S_0 , S_1 , S_2 and S_4) , the four Stokes parameters are defined in terms of the electric field components [11] :

$$\begin{cases} S_0 = A_x^2 + A_y^2, \\ S_1 = A_x^2 - A_y^2, \\ S_2 = 2A_xA_y\cos\varphi, \\ S_3 = 2A_xA_y\sin\varphi, \\ \varphi = \varphi_x - \varphi_y, \end{cases} \tag{2}$$

where S_0 denotes the total intensity of the light wave; S_1 denotes the linearly polarized light component in the horizontal direction; S_2 denotes the linearly polarized light component in the 45° direction; S_3 denotes the right

circularly polarized light component. When there is a light orthogonal to the above polarized light, the corresponding parameter is negative.

Degree of polarization (DOP) is a parameter that describes the polarization state of a light wave. It is the ratio of the polarization component of the light wave to the total amplitude of the light wave, and the formula is as follows:

$$DOP = \frac{\sqrt{S_1^{\,2} + S_2^{\,2} + S_3^{\,2}}}{S_0} \tag{3}$$

and its meaning is to determine whether the light is fully polarized. In general, $0 \le DOP \le 1$. When $DOP = 0$, the light wave is completely unpolarized light, that is, natural light; when $0 < DOP < 1$, the light wave is partially polarized light; when $DOP = 1$, the light wave is completely polarized light. The Stokes parameters are not orthogonal to each other, and there is an inequality relationship between the four parameters:

$$S_1^{\,2} + S_2^{\,2} + S_3^{\,2} \le S_0^{\,2} \tag{4}$$

where the equal sign holds for fully polarized light. In order to eliminate the effect of light intensity, the Stokes parameters are normalized. The normalization is usually done by dividing the parameters S_1, S_2 and S_3 by S_0. The SOP can be determined by taking S_1, S_2, S_3 as the coordinate axes and 1 as the radius on a sphere, which is also called Poincare sphere.

B. Stokes parameters of Bending eavesdropping

Bending eavesdropping is an attack method to obtain optical signals by stealing the weak leakage light in the transmitted optical signals and analyze and decode them. Specifically, when an optical fiber is bent, weak leakage light is generated inside the fiber, which can be captured and analyzed by an eavesdropper to obtain the transmitted information. The strength of bend eavesdropping is related to the bend radius. As the bend radius decreases, the more light leakage in the fiber, the easier it is for eavesdroppers to intercept and steal communication information. In addition, the bend radius also affects the transmission loss in the fiber, which can affect the communication quality and distance.

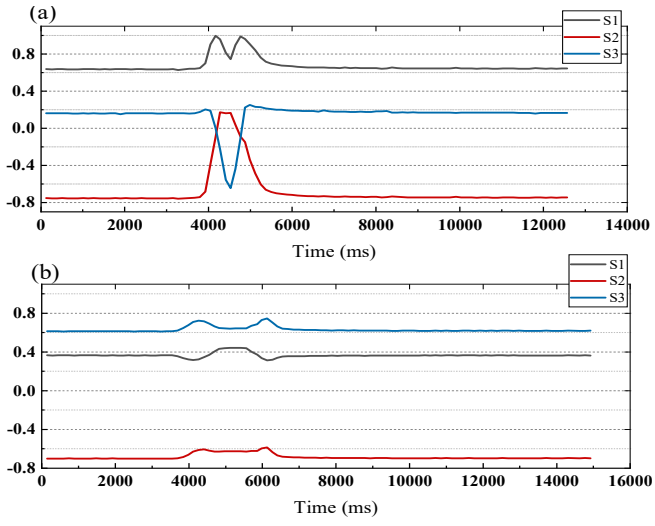

Fig. 1. Changes in Stokes parameters due to (a) strong bending (b) weak bending eavesdropping.

The process of fiber bending causes a change in fiber geometry, which in turn causes a change in SOP. Changes in SOP have a significant impact on transmission performance, causing problems such as polarization rotation, phase delay and optical intensity attenuation of the optical signal, which can lead to increased distortion and errors in the optical signal and reduce transmission quality. Therefore, bending eavesdropping with different intensities, meaning different bending radii, can have different effects on the eavesdropper and transmission quality. As shown in Fig. 1, different strengths of bending eavesdropping are experimentally measured to cause different changes in the Stokes parameters. Fig. 1 (a) is a strong bending eavesdropping with a bending radius of 0.5 cm, and Fig. 1 (b) is a weak bending eavesdropping with a bending radius of 5 cm. Therefore, it is feasible to identify multi-intensity bending eavesdropping based on the variation of Stokes parameters.

C. Bending eavesdropping detection process

When measuring the Stokes parameters of multi-intensity bending eavesdropping, the situation as shown in Fig. 2(a) occurs. The complex and strong uncertainties in the variations of the three sets of parameters are not conducive to the identification of different intensity bending. Therefore, in this paper, the angular velocity of SOP variation is chosen as the identification parameter of multi-intensity bending, which is calculated as Eq. (5) [10]:

$$\theta_n = \cos^{-1}\left(1 - \frac{\left|\vec{S}_n - \vec{S}_{n-1}\right|^2}{2}\right) / \Delta t \tag{5}$$

$$\vec{S}_n = (S_{1n}, S_{2n}, S_{3n}) \tag{6}$$

where $\vec{S}_n$ and $\vec{S}_{n-1}$ are the measured adjacent Stokes parameter vectors and Δt is the sampling period of the measured Stokes parameter.

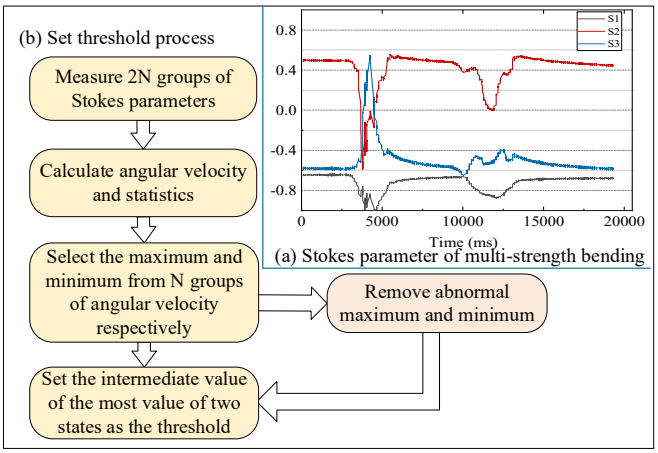

Fig. 2. (a) Multi-intensity bending eavesdropping Stokes parameters. (b)

After obtaining the angular velocity, this paper uses a threshold judgment to identify the multi-intensity bending eavesdropping. The flow of setting the threshold value is shown in Fig. 2(b). First, N sets of strong bending eavesdropping and weak bending eavesdropping are performed separately, measuring the Stokes parameters and Select the maximum value of angular velocity from each eavesdropping session as the decision parameter for this

session, and statistically analyze the distribution of maximum angular velocities for N groups of strong bending and N groups of weak bending separately. Then, select the maximum and minimum values from the statistically analyzed N groups of strong and weak bending angular velocities, respectively. Note that this step requires the removal of unusual extremes caused by operational or environmental fluctuations, such as the presence of much higher angular velocities in weak bending eavesdropping than in other weak bending, which may be due to operational errors. $V_{s\_\min}$ and $V_{s\_\max}$ are the minimum and maximum values of the angular velocities from N groups of strong bending, respectively, while $V_{w\_\min}$ and $V_{w\_\max}$ are from N groups of weak bending. Finally, set the thresholds for normal state and weak bending $D_1 \in (0, V_{w\_\min})$, choosing intermediate values from 0 to $V_{w\_\min}$; set the threshold values for weak and strong bending $D_2 \in (V_{w\_\max}, V_{s\_\min})$, choosing intermediate values from $V_{w\_\max}$ to $V_{s\_\min}$. The threshold values can be rounded to the nearest integer. The test data is then used to detect and identify multi-intensity bending eavesdropping according to the thresholds that have been set.

III. Experimental Setup and Result Analysis

A. Experimental setup

The experimental setup is shown in Fig. 3(a). A 10GHz bandwidth arbitrary waveform generator (AWG) generates a 16QAM signal, which is converted into an optical signal through an IQ modulator. The signal is amplified by an amplifier and transmitted over a 20km optical fiber, and then received by a polarization measurement system at the receiving end. The polarization measurement system used in this paper is PSGA-101A, and eavesdropping was conducted by bending the optical fiber at a distance of 20km. The SOP data of the signal measured by PSGA-101A is shown in Fig. 3(b), which includes the measurement time, four Stokes parameters, and the DOP.

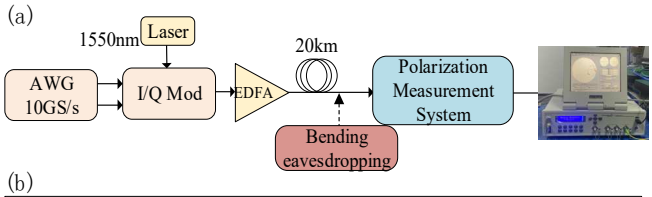

(b)

--Time--	S0	S1	S2	S3	DOP
127	-1.1017	-0.9387	-0.0612	0.3394	0.9784
128	-1.0989	-0.9388	-0.0599	0.3392	0.9794
128	-1.1055	-0.9389	-0.0619	0.3385	0.9782
129	-1.1059	-0.9386	-0.0598	0.3399	0.9783
130	-1.1046	-0.9387	-0.0592	0.3398	0.9782

Fig. 3. (a) Bending eavesdropping experimental setup. (b) Polarization

In this paper, the bending radius of strong bending is set to 0.5 cm and the bending radius of weak bending is set to 5 cm. A total of 230 sets of the SOP data are measured, including 100 sets of weak bending, 100 sets of strong bending, and 30 sets of normal state. Among them, 50 sets of weak bending and 50 sets of strong bending are used to set the threshold, and the remaining 130 sets of data are used for testing.

B. Result analysis

Fig. 4 shows the angular velocity variation for the normal state, weak bending and strong bending, respectively, with a measured duration of 25000ms. As can be seen in Fig. 4(a), the angular velocity fluctuates slightly in the normal state, which is due to the environment, but it remains overall around 5 rad/s. Fig. 4(b) shows the angular velocity of a weak bending eavesdropping process. We choose the maximum value of the whole process as the identification parameter of this eavesdropping, and from this figure we can conclude that the maximum angular velocity of this weak bending is about 45 rad/s. The angular velocity of the strong bending eavesdropping is shown in Fig. 4(c), and the maximum angular velocity of this eavesdropping is around 200 rad/s.

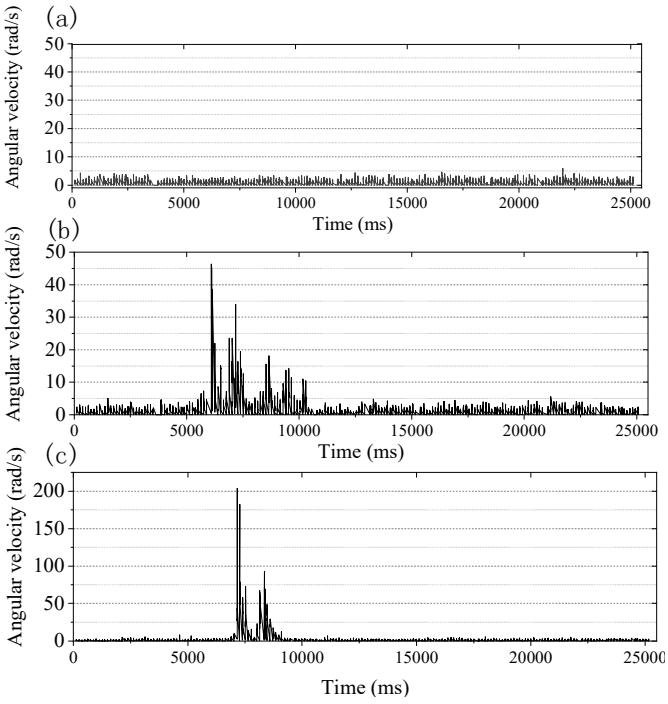

Fig. 4. (a) Angular velocity of the normal state. (b) Change in angular velocity for one weak bending eavesdropping. (c) Change in angular velocity

TABLE I. Weak bending and strong bending angular velocity statistics

Angular velocity	Total N	Average	Minimum	Maximum
Weak bending	50	34.7639	18.9397	55.4361
Strong bending	50	186.4947	100.4008	438.9062

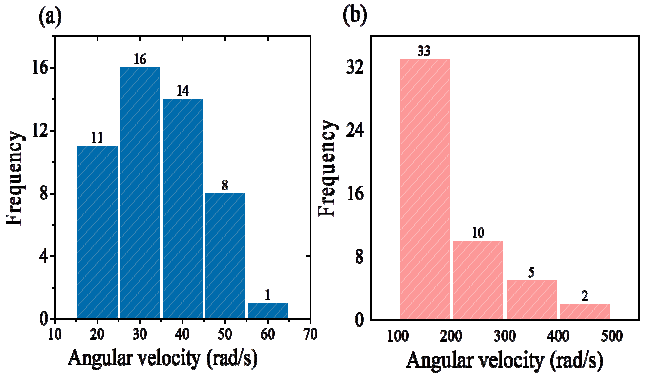

Fig. 5. The histogram of angular velocity statistics for 50 groups under (a)weak bending (b) strong bending.

The angular velocity is calculated using Eq. (5) for the 50 groups of weak bending and 50 groups of strong bending Stokes parameters measured in the experiment. Select the maximum value of angular velocity during each eavesdropping process and perform statistical analysis on them as shown in Table I and Fig. 5. It can be seen from Fig. 5 that the angular velocity of the 50 groups of weak bending is mostly in the range of 20-40 rad/s, with a minimum value of 18.9397 and a maximum value of 55.4361. Most of the angular velocities of the 50 groups of strong bending were in the range of 100-200 rad/s, with a minimum value of 100.4008 and a maximum value of 438.9062. Since the SOP is very sensitive to changes in fiber geometry, the range of SOP variation for strong bending can be relatively large. According to the data in Table I and the threshold setting process in Fig. 2(a), this paper sets the angular velocity in 0-10 rad/s as the normal state, 10-80 rad/s as the weak bending state, and above 80 rad/s as the strong bending.

TABLE II. Test data identification results.

Fiber Status/Frequency	Identified fiber status		
	Normal	Weak bending	Strong bending
Normal /30	27	3	0
Weak bending/50	0	47	3
Strong bending/50	0	0	50

The identification results of 130 sets of test data are shown in Table II. The angular velocities of 30 sets of normal states, of which 27 sets are identified correctly and 3 sets are identified as weak bending; the angular velocities of 50 sets of weak bending states, 47 sets are identified correctly and 3 sets are identified as strong bending; the angular velocities of 50 sets of strong bending states are all identified correctly. The overall multi-intensity bending eavesdropping recognition rate is 95.38% correct.

The results show that the correct identification rate of the secure state and weak bending is lower compared with the strong bending. In the secure state, although no eavesdropping operation is performed on the fiber, the perturbation of the environment still has a slight effect on the SOP. Further research can be conducted next for the identification of secure state and weak bending to improve the correct rate of the whole scheme.

IV. CONCLUSION

In this paper, we propose a polarization-based multi-intensity fiber bending eavesdropping detection and identification scheme. The SOP parameter of the signal is measured experimentally, and the angular rate of the polarization rotation is calculated using the SOP parameters. After experimental data verification, the identification of bend eavesdropping for different intensities is achieved with 95.38% accuracy.

ACKNOWLEDGMENT

This work is supported in part by NSFC (61831003, 62021005, 62101063), Beijing Natural Science Foundation(4232011), and Project of Jiangsu Engineering Research Center of Novel Optical Fiber Technology and Communication Network, Soochow University(SDGC2117).

REFERENCES

[1] A. L. Feffer, “Comprehensive security strategy for all-optical networks,” in Diss. Massachusetts Institute of Technology, 2015.

[2] T. Sasai, M. Nakamura, E. Yamazaki, S. Yamamoto, H. Nishizawa and Y. Kisaka, "Digital Backpropagation for Optical Path Monitoring: Loss Profile and Passband Narrowing Estimation," in *2020 European Conference on Optical Communications (ECOC)*, Brussels, Belgium, 2020, pp. 1-4.

[3] S. Gleb, P. Konstantin, J. Luo and B. Zheng, "Fiber Link Anomaly Detection and Estimation Based on Signal Nonlinearity," in *2021 European Conference on Optical Communication (ECOC)*, Bordeaux, France, 2021, pp. 1-4.

[4] C. Natalino, M. Schiano, A. Di Giglio, L. Wosinska and M. Furdek, "Experimental Study of Machine-Learning-Based Detection and Identification of Physical-Layer Attacks in Optical Networks," in Journal of Lightwave Technology, vol. 37, no. 16, pp. 4173-4182, 15 Aug.15, 2019.

[5] H. Song, Y. Li, M. Liu, K. Wang, J. Li, M. Zhang, Y. Zhao and J. Zhang, “Experimental study of machine-learning-based detection and location of eavesdropping in end-to-end optical fiber communications,” in Optical Fiber Technology, 2022, 68, 102669.

[6] T. Tanaka, S. Kuwabara, H. Nishizawa, T. Inui, S. Kobayashi and A. Hirano, "Field Demonstration of Real-Time Optical Network Diagnosis using Deep Neural Network and Telemetry," in 2019 Optical Fiber Communications Conference and Exhibition (OFC), San Diego, CA, USA, 2019, pp. 1-3.

[7] T. Tanaka, T. Inui, S. Kawai, S. Kuwabara and H. Nishizawa, "Monitoring and diagnostic technologies using deep neural networks for predictive optical network maintenance [Invited]," in Journal of Optical Communications and Networking, vol. 13, no. 10, pp. E13-E22, October 2021, doi: 10.1364/JOCN.424428.

[8] G. MacDonald, “Detecting eavesdropping activity in fiber optic networks,” in PhD Dissertation, The University of Oklahoma, Oklahoma, 2012.

[9] R. El Hajj, G. MacDonald, P. Verma and R. Huck, "Implementing and testing a fiber-optic polarization-based intrusion detection system", in *Optical Engineering*, vol. 54, pp. 096107-096107, 2015.

[10] D. Charlton, S. Clarke, D. Doucet, M. O'Sullivan, DL. Peterson, D. Wilson, G. Wellbrock, M. Bélanger, "Field measurement of SOP transients in OPGW with time and location correlation to lightning strikes", in *Opt. Exp.*, vol. 25, no. 9, pp. 9689-9696, May 2017.

[11] A. Kumar and A. Ghatak, “The Stokes parameters representation,” in Polarization of Light with Application in Optical Fibers, pp. 97–119, SPIE Press, Washington , 2011.